AIChE

Predictions of Porosity and Fluid Distribution Through Nonspherical-Packed Columns

Richard Caulkin, Xiaodong Jia, Michael Fairweather, and Richard A. Williams
Institute of Particle Science and Engineering, School of Process, Environmental and Materials Engineering, University of Leeds, Leeds LS2 9JT, UK

DOI 10.1002/aic.12691
Published online July 7, 2011 in Wiley Online Library (wileyonlinelibrary.com).

For beds comprised randomly arranged nonspherical particles, the prediction and understanding of the packing characteristics and subsequent fluid flow through the resulting porous media is a longstanding problem for chemical and process engineers. This paper presents the application of a digital modeling approach to particle packing, in which no more than elementary physical concepts are used, with the model using collision points to predict trends in bed structures of particles of different geometry. Lattice Boltzmann modeling (LBM), coupled to the output of the packing model, is used to subsequently assess velocity distribution through the generated structures. Simulation results are compared with data available from the literature, as a means of model validation, where it is demonstrated that the combined approach of the digital packing algorithm and LBM provide a modeling capability that is of value to a range of engineering applications. © 2011 American Institute of Chemical Engineers *AIChE J,* 58: 1503–1512, 2012
Keywords: chemical reactors, packed bed, simulation, voidage, fluid velocity distribution

Introduction

From the many studies into packed beds, it has been established that bed structure within packed columns is essentially affected by four key parameters, namely, the particles (shape and size distribution), the container (shape and the related tube-to-particle diameter ratio), the method of packing (rate, intensity, bed inlet, and outlet conditions), and the treatment of the final packing matrix (vibration, shaking, and compression).

Packed beds contained within cylindrical vessels are widely used in the chemical and process industries, and because of their high surface area ratios, they are the dominant type of reactor used for industrial heterogeneous catalytic reactions. As such, a substantial body of work has already been undertaken in an attempt to quantify the structural properties of packed beds and the transport processes through them to facilitate the design of more efficient unit operations. Numerical modeling using computational fluid dynamic calculations (CFD)[1–5] has advanced to the stage, where it now has the potential to become a valuable tool in the field of research and design for many disciplines, including that of chemical reactors. In recent studies, the generation of the packing and the simulation of fluid flow have been combined with subsequent simulation of pore-scale tracer dispersion[6–8] or a subsequent simulation of a chemical reaction.[9,10] However, the majority of these studies have utilized the packing of spheres or spheroids in the consideration of flow characteristics.

As packed beds are naturally associated with varying degrees of randomness,[11] influenced by the specific structural and geometric make-up, the internal free channels present within individual packed structures should not be disregarded when investigating flow distribution within packed columns.[12–15] There is great interest in practical models for use in the improved design of systems such as fixed bed

Correspondence concerning this article should be addressed to R. Caulkin at r.caulkin@leeds.ac.uk.

reactors, where fluid dynamics are of main concern. This holds especially for the prediction of the transport of reagents within the packing produced by nonspherical objects. A significant step for computational modeling of fluid flow, therefore, is the necessity for an accurate and reliable method of generating the three-dimensional geometric structures of beds packed with realistic, nonspherical shaped particles.

Traditionally, there are several key methods, whereby this may be achieved. The longest standing is that of direct experimental investigations[16–18] from which numerical correlations can be derived.[19–21] These are largely limited to specific bed types, however, because of the restricted nature of the experimental data used in their derivation, and often require the use of correction factors in an attempt to make them more adaptable. A more recent, tomographic-based method is to obtain a three-dimensional image of a real bed structure by utilizing advances in 3D imaging technology. Numerous studies using modern, noninvasive analysis methods, such as X-ray microtomography (XMT)[22–25] and nuclear magnetic resonance imaging (MRI) techniques,[26,27] have been reported. The major limitation of these methods, however, is the high financial cost of such scanners. With continued advances in computational power, an increasingly effective method of deriving the complete 3D bed structure is by the use of numerical simulation techniques.[2,28–31] Of the recent models proposed in the literature, many can predict sphere-/spheroid-packed beds with good levels of accuracy, and several are capable of handling more complex, nonspherical particles. However, the majority of these are found to be unsuccessful in the accurate prediction of macroscopic properties when compared with experimentally measured beds of corresponding geometry due to the challenges encountered in representing large numbers of randomly orientated particles.

This work extends earlier studies by the authors. In previous papers,[32,33] the focus concerned simulation of the structure of packed beds, without fluid flow through them. A digital-based packing algorithm was introduced,[32] which uses collisions to determine particle movements and rotation, without sacrificing the advantage of simulation speed provided by a previous version of the packing model.[34] Simulations of packing structure obtained using this model were compared with experimental data for the case of solid and hollow monosized equilateral cylindrical pellets within conventional and shell-side containers, with the particles residing on the outer side of either single or multiple tubes contained within the shell in the latter case, with good agreement found between measurements and predictions. These comparisons were subsequently extended,[33] with predictions compared with a variety of packing structures made up of nonspherical objects (cylinders, pall-rings, and hama beads), with structure measurements obtained from XMT scans of the beds. Simulations were performed using the previous collision-guided packing algorithm, as well as a discrete element-based method introduced to allow incorporation of the effects of particle interaction forces. This work demonstrated, through an analysis of pellet orientation distribution in the near-wall region, that particle–particle and particle–wall interactions cannot be ignored if realistic packing structures are to be obtained by simulation. Extension of this work to examine fluid flow through packed beds using lattice Boltzmann modeling[35] (LBM) has also been reported[36] in a preliminary study. The latter work, which considered sphere-, cylinder-, and ring-packed beds, only presented a single aspect ratio bed for each case, which precluded a comparison of the effects of pellets with different tube-to-particle diameter aspect ratios, as is considered in this work.

This work considers the structural aspects of packed beds given their influence on fluid flow through a bed. It draws on the experimental data sets examined previously[32] for validation purposes, although different beds packed with different objects are considered herein, in addition to previously unused data from the open literature. Therefore, the work described below considers solid cylinders, rings, and trilobe pellets packed in conventional beds, with the study extended to include fluid flow through the packed structures for a variety of tube-to-particle diameter aspect ratios. Predicted flow results are also compared with experimental data from the literature collected using a variety of analytical methods. The purpose of this combined study is to demonstrate that together, the two lattice-based packing and fluid flow techniques have the potential for use as a software tool of value in the design and optimization of packed columns.

Numerical Simulation Methods

Packing generation model

The algorithm, called DigiPac,[34] is a PC-based tool that uses a digital approach toward the movement and packing of objects. As digitized images are utilized, objects, regardless of complexity, are represented as coherent collections of pixels or voxels. This ''pixelation'' (2D) or ''voxelation'' (3D) of particles, and of the packing space, is the basis of the algorithm, which permits complex or arbitrary shapes to move one step at a time, within the boundaries of the packing space (which is mapped over a cubic-lattice grid). As the packing space is also digitized and represented in the same way, using a container of complex geometry presents no additional difficulties. The version of the DigiPac algorithm used in this work uses particle collisions to guide particle movements over the 3D grid by means of probability (Collision Guided Packing or DigiCGP).[32] As particles reside and move on a grid, collision and overlap detection is a simple matter of detecting whether two objects occupy the same site(s) at a given time, rather than having to compute and test intersections between objects which are usually the most computationally expensive part of particle packing simulations. As a particle moves only one grid space at a time, the overlap detection procedure ensures that one particle will not jump over another during packing.

To simulate the individual collision forces that act on every particle would come at a high computational cost. However, for beds that consist of relatively large and more or less identical pellets, and for trend finding exercises, a quicker, albeit less accurate, solution is more desirable. In DigiCGP,[32] collision points are identified in the lattice grid and each pair of colliding voxels is assigned a nominal impact force of one. For torque calculation, the direction of the nominal impact force is taken to be normal to the contact face of the colliding pair of voxels. The net torque vector is

subsequently used as the axis of particle rotation in the following step. The angle of rotation is still random, but is capped to give a maximum swept distance of no more than a few pixels during the rotation. To calculate the net force, the direction of an impact force is taken to be along the line joining the collision point and the center of gravity of each particle. For translational movement, the net collision force is normalized against the largest component, so each force component is now between 0 and 1. Then, this is then used as the probability of moving the particle by at most one grid cell at a time along each principal axis in the lattice grid. Thus, instead of being completely random, the directions of particle movement and rotation are guided by collisions. It should be noted that the above treatment does not include voxel-level friction or any other forces tangential to a contact. Particle-level friction is partially accounted for by the roughness of the digital surfaces. The method also neglects inertia effects as particle velocity is neither calculated nor stored. All these omissions are for the sake of computational speed and result in a relatively fast simulation time (typically <1 h for the reported results). A version of the packing model in which friction and inertia effects are considered in the determination of torque (DigiDEM) has been reported.[33] Comparison of the generated structures (from DigiDEM and DigiCGP) identified that for systems involving large and identical objects, the simplification described above, and used in this work, is justifiable and acceptable, resulting in quantitative predictions in terms of packing structure. Further description and validation of the code implementation is given in recent publications.[32–34]

Lattice Boltzmann fluid flow model

LBM is frequently used in the prediction of fluid flow phenomena because of a number of advantages it has over conventional continuum approaches. For flow simulation through packed beds, two distinct practical advantages led to its adoption in this work. First, the method is relatively straightforward to implement as a software program, and can easily be parallelized to make the best use of today's computing facilities. For the single time scheme model, LBM is also generally much faster than CFD in dealing with cases involving complex boundary geometries. Second, it is lattice based and thus can directly use as its input, digitally specified structures—no matter how complex the structures may be. Such structures can be obtained either from computer-based simulation techniques such as DigiPac or through tomographic imaging techniques such as XMT and MRI.

LBM is directly descended from the discretization and solution of the Boltzmann equation, which describes population distribution in time and space. It breaks physical space into a large number of nodes or sites (typically $\sim 10^6$ or more) on a regular lattice grid. At each node a set of mass probability distributions is used to represent the fluid. In each time step, the distributions translate from node to node along fixed velocity vectors, where they then undergo simple collisions that conserve physical properties such as mass and momentum.

Different implementation schemes exist. The one used in this work is the so-called Bhatnagar-Gross-Krook (BGK) single relaxation time D3Q19 scheme,[37] with software implementation in which flow is driven by a constant body force,[38] equivalent to a constant pressure gradient. In this scheme, the evolution of the particle distribution function f_i satisfies

$$\underbrace{f_i(x+e_i,t+1)=f_i(x,t)}_{\text{translation}}\underbrace{-\frac{f_i(x,t)-f_i^{\text{eq}}(x,t)}{\tau}}_{\text{collision}} \tag{1}$$

where x is a node position vector, e_i is the lattice velocity vector ($i = 0, 1,\ldots 18$ for D3Q19), t is time, f_i^{eq} is the equilibrium distribution, and τ is a relaxation parameter, which relates to the kinematic viscosity, v, by

$$\tau = 3v + \frac{1}{2} \tag{2}$$

It is customary in LBM formulations to rescale parameters such that the time step, grid size, and magnitude of orthogonal velocities are all, numerically, 1. As such, everything is expressed in lattice units. It is also customary that Eq. 1) is implemented in two steps. The second term on the RHS is determined in one step, the collision step; with the remaining terms determined in the translation (also called streaming) step. The equilibrium distribution,[39] f_i^{eq}, is given by

$$f_i^{\text{eq}} = w_i\rho\left[1+\frac{3}{c^2}(e_i\cdot u)+\frac{9}{2c^4}(e_i\cdot u)^2-\frac{3}{2c^2}(u\cdot u)^2\right] \tag{3}$$

The weighting factor w_a is 1/3 for $i = 0$; 1/18 for the six orthogonal directions, and 1/36 for the 12 diagonal directions. Note that $e_0 = 0$, so Eq. 3 for $i = 0$ is simplified with the second and third terms in the square brackets set to zero. The macroscopic velocity u is an average of the microscopic (i.e., lattice) velocities weighted by the directional density functions:

$$u = \frac{1}{\rho}\sum_i f_i e_i \tag{4}$$

The macroscopic fluid density is simply the sum of the density functions:

$$\rho = \sum_i f_i \tag{5}$$

Given that in LBM the pressure is related to density[37] as $p = \rho/3$, and the equivalence between pressure gradient and body force,[37] the driving (body) force, $f_{b,}$ for flow can be implemented by adding a perturbation term, equal to $f_b\tau$, to the macroscopic velocity u when calculating the equilibrium functions f_i^{eq} during the collision step.[40]

The PC used for the simulations was a dual AMD Opteron 248 CPU (2.2 GHz) 8 GB RAM machine running the Linux operating system (64-bit version of SuSE 9.1). Typical simulation times, including the generation of packing structures, were ~3 h, with the code using multithreads to run on the two processors simultaneously.

Validation Methods

The ability of the described packing algorithm is investigated for cylinder-, ring-, and trilobe-packed beds. The

Table 1. Physical Dimensions of the Beds Investigated

Particle	Particle Diameter (mm)	Particle Length (mm)	Internal Hole Diameter (mm)	Container Diameter (mm)	Aspect Ratio (d_t/d_p)
Cylinder 1	6	6	–	50	8.3
Cylinder 2	8	8	–	80	10.0
Ring 1	10	10	5.3	50	5.0
Ring 2	8	8	6.0	80	10.0
Trilobe packing	1.3	6	–	40	30.8

container-to-particle diameter aspect ratios investigated are given in Table 1. The first part of this work is concerned with reaching an accurate and realistic description of the structure of beds packed with different shaped pellets, both in the region close to the vessel wall and in the bulk of the bed for monodispersed columns. The near-wall region, up to one particle diameter into the packing, is widely regarded to be one of the most important regions of a packed bed in terms of fluid channeling.[40] To determine the degree to which packing shape and size influence wall effects within the simulations a range of aspect ratios are investigated. Although it is not commonplace to find industrial packed beds with aspect ratios below about 6.0, an interest in such cases cannot be excluded because of their relevance to pilot plant applications.

The second part of this work investigates the steady state flow patterns, namely the axially and circumferentially averaged velocity profiles in the radial direction, as influenced by the generated packing structures. Therefore, the objective of the flow simulations is to compare the resulting velocity distributions with local structural analysis to assess corresponding similarities, in addition to comparing predicted velocity distributions with those reported in the literature for geometrically similar beds.

LBM simulations were performed on the packing structures for the flow conditions considered by Bey and Eigenberger,[41] Giese et al.,[42] and Mantle et al.[43] For the setup of the simulations, a suitably sized matrix ($400 \times 400 \times 500$) was used for each bed, with one quarter of the bed height removed from each end before the LBM simulations being undertaken. This was done as the random nature of the packing in these regions is not representative of the packing structure as a whole. Therefore, the truncated sections of the packing provided for the collection of steady state statistics by avoiding end effects.

Investigation of the predictive ability of the complete digital algorithm was carried out by comparison of numerical simulation results with experimentally derived data from the published domain. Despite the many publications on flow through packed columns, systematic investigation of low aspect ratio beds is scarce, especially for beds consisting of nonspherical particles. The predictions presented herein are therefore compared with published experimental data from a range of sources where local voidage and fluid velocity profiles are known; Bey and Eigenberger[41] used an approach whereby information on velocity distribution inside the packing was implied by the use of measurements carried out a short distance below the bed, with the structure of the outlet flow preserved by a monolith. The extrapolation of these values to the inside of the packing, however, has been questioned by a number of researchers because of the suspicion that flow profiles evaluated below the packed bed are mainly shaped by the last one or two particle layers, so any recorded velocity profiles are not truly representative of the complete bed structure, but only the last few layers of particles. However, although the flow values may not be representative in terms of the entire packing structure of a bed, they do allow a qualitative assessment of velocity distribution for beds of corresponding geometry. More recently, the use of increasingly advanced measurement techniques such as laser Doppler anemometry (LDA) and MRI has permitted the measurement of local velocities inside the packing. For validation of the present simulations, data from Giese et al.[42] (LDA) and Mantle et al.[43] (MRI) were used. Giese et al.[42] performed LDA-measurements using packings of equilateral cylinders and Raschig ring pellets inside low aspect ratio columns, obtaining data for both the local packing structure and subsequent fluid velocities inside the packed beds. Experimental data on a single vertical measurement plane (i.e., axially averaged, but at a certain circumferential position) are compared with axially and circumferentially averaged radial velocity profiles from the present simulations. Sharma et al.[44] and Mantle et al.[43] presented packing and subsequent flow analysis (using MRI) on cylinder- and trilobe-packed columns.

Results and Discussion

The predictions presented show time averaged results that are axially averaged over the complete height of the columns. The dimensionless velocity distributions presented in Figures 1–3 were obtained by normalizing measured velocity within the packed beds (mm s^{-1}) with superficial liquid velocity (mm s^{-1}). Because of the different methods used to assess quantities between measured and predicted values, and between the experimental measurements of one researcher and another, it is to be expected that there will be variances between the predictions and the data. Therefore, the aim of the simulations is to attempt to predict the trend and extent of fluctuations for different pellet shapes and pellet/column size ratios.

Analysis of cylinder-packed structures

It is found (Figure 1) that the void fraction distributions of the simulated cylinder-packed beds are in good agreement with results gained from experimental investigations, particularly in the near-wall regions (≤ 1.0), where a reasonable fit is observed for each bed considered. In an attempt to minimize any inconsistencies caused by the random nature of the packing, simulated mean values of four trial runs per bed type are presented. However, in each case, it is important to note that an exact replication of the bed structure is not possible as the packing varies because of the arbitrary particle orientation, despite the influence of the retaining wall which often promotes particle ordering. From previous studies,[32] this number of trials has been demonstrated to be adequate for attaining reproducible results from the packing algorithm. Error bars showing the spread of the individual simulated runs are also shown.

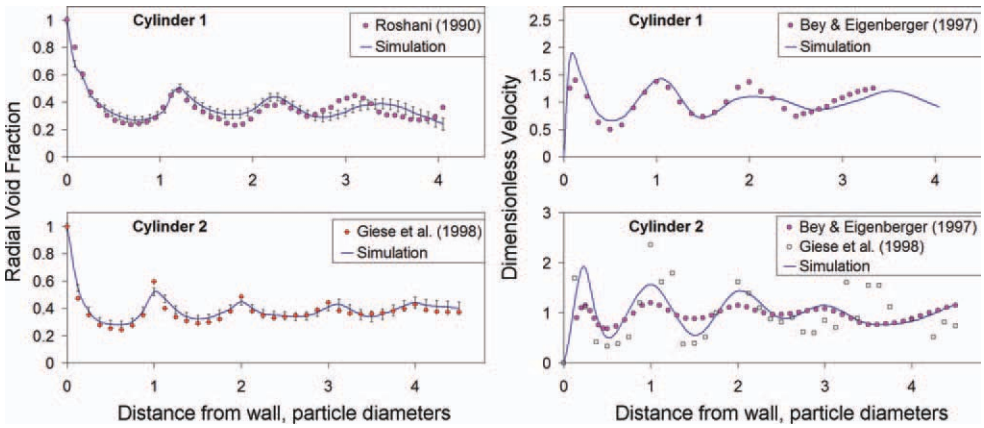

Figure 1. Averaged radial voidage (left-hand side column) and averaged radial velocity (right-hand side column) for bed of cylinders of aspect ratios $d_t/d_p = 8.3$ (top) and $d_t/d_p = 10.0$ (bottom).

Predicted voidage shows error bars associated with individual values of repacked beds. [Color figure can be viewed in the online issue, which is available at wileyonlinelibrary.com.]

For the plot labeled "Cylinder 1," no experimental packing data were presented for the bed for which fluid flow data were obtained. Therefore, there is no means of being sure that the simulated bed structures produced by the packing algorithm qualitatively agree with the experimentally derived ones through which the fluid was passed. However, the ability of the packing method in quantitatively predicting the local porosity of cylinder-packed columns has been demonstrated elsewhere.[32] An example of one of these simulated bed structures, and its adherence to experimentally measured radial voidage data[45] in a bed of similar aspect ratio to that used for flow prediction, is presented in Figure 1. The experimental radial voidage distributions are seen to correlate well with predicted results. However, this is far from an ideal situation for model validation, although the packing data presented do demonstrate the potential of the model as a predictive tool, despite the voidage and flow data originating from two different bed sources in this particular case.

Measured fluid velocity data[41,42] for flow through cylinder-packed columns are also compared with LBM predictions in Figure 1. The radial distributions of axial flow are scaled with the velocities from the empty beds for both experiment and simulation. There exists good qualitative agreement between measured and predicted results, particularly for "Cylinder 1," where the data are closely reproduced at a distance of between $\geq 0.25d_p$ and $\leq 1.75d_p$ from the containing wall. For "Cylinder 2," however, the main differences between measured and predicted velocity profiles exist close to the container wall, specifically within the first $2.5d_p$. This could be attributed to the shortcomings of the experimental method,[40] whereby fluid velocity was measured exiting the bed at different radial positions. The dependability of these data in terms of their ability to represent the flow through the bed has been questioned, and the velocity distribution shown in Figure 1 may have been influenced significantly by the final few layers of particles.

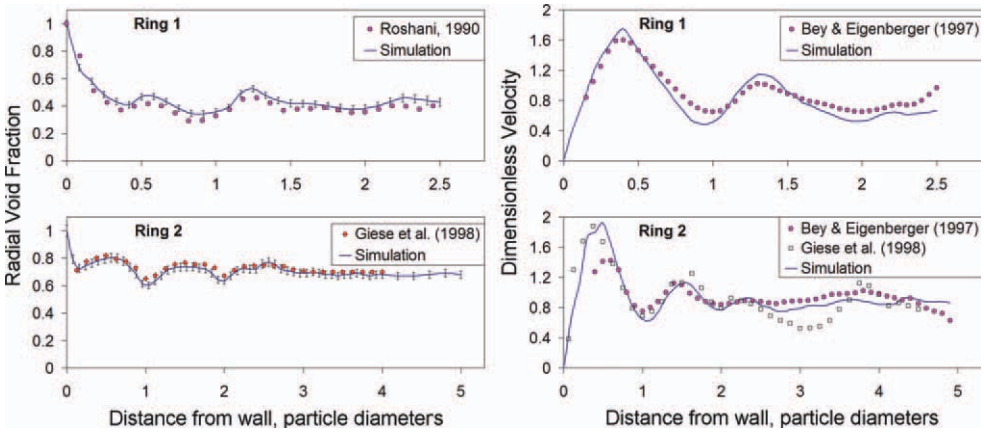

Figure 2. Axially averaged radial voidage (left-hand side column) and averaged radial velocity (right-hand side column) for bed of rings of aspect ratios $d_t/d_p = 5.0$ (top) and $d_t/d_p = 10.0$ (bottom).

Predicted voidage shows error bars associated with individual values of repacked beds. [Color figure can be viewed in the online issue, which is available at wileyonlinelibrary.com.]

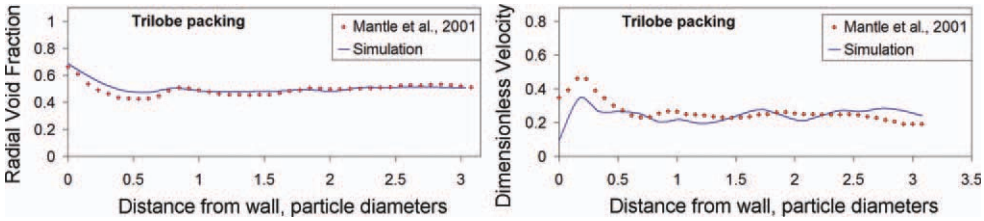

Figure 3. Axially averaged radial voidage (left-hand side column) and averaged radial velocity (right-hand side column) of trilobe packing for $d_t/d_p = 30.8$.

[Color figure can be viewed in the online issue, which is available at wileyonlinelibrary.com.]

Alternatively, the packed structures of the two beds (measured and predicted) may be sufficiently different, leading to varying oscillatory amplitudes of flow velocity. The frequencies of the measured and predicted oscillatory waves are, however, in qualitative agreement. This suggests that the size and shape of the packing material may predominantly govern the oscillatory wave in terms of the position of flow minima and maxima at specific distances from the wall, but it is the manner and order in which these particles are packed that determines the quantitative velocity through the bed at these minimum and maximum points.

The agreement of the predicted velocity distribution with the experimental results[42] is also reasonable (Figure 1), particularly $<1d_p$ from the containing wall. However, further into the packing structure ($>3.0d_p$) the measured results[42] display a large degree of scatter, particularly in the center of the bed. Minor discrepancies commonly observed in the central region of a bed can generally be attributed to the increased random nature of the packing because of the absence of any wall structure. For cylinder-packed beds, however, this may be further exacerbated by the geometry of the particles in terms of random pellet orientations. It is also suspected in this case that differences in data collection methods, and the methods used to pack the beds, could account for some of the discrepancies. In terms of packing the beds, little information is given on the methods used by the researchers, who undertook the experimental work. For the predicted beds, the method aimed to simulate a poured random packing, which is a well-established method for loading packed columns. This was achieved by adding a small number, or batch, of particles, enough to form a complete layer one particle thick at the base of the column. The particles were allowed to "rain" down over the circular area of the column, collide, rotate and rearrange during free-fall before settling to form a close packing by means of a rebounding probability (0.3). Once every particle in this layer was stationary, another batch was added and allowed to settle in the same way. This was repeated until the column contained a sufficient number of particles, so that the packing reached the full height of the container. For data collection, Giese et al.[42] utilized a laser Doppler anemometry technique whereby velocity was measured over a single cross section of the bed at a predetermined height in the column. In comparing the measured and predicted results, the reliability of the LDA technique is not in question. However, the fact that only one cross section was averaged to generate the data shown in Figure 1 means that the number of samples used may not give a representative picture of the overall flow distribution through the complete bed structure. Consequently, the experimental data sets used in Figure 1 differ both from one another and from predictions, because in the simulations, the fluid velocity was calculated for every cross section, one pixel in height, and was then averaged over the bulk section of the bed, allowing the derivation of a flow velocity that is more representative of the bed structure. Use of this technique demonstrates the advantage of the numerical simulation approach over that of experimental measurement in terms of the amount of information and ease with which it can be extracted from individual beds, as well as highlighting the difficulties inherent in obtaining reliable velocity measurements within packed beds.

Analysis of ring-packed structures

As with cylindrical packings, structural data for one of the beds ($d_t/d_p = 5.0$), corresponding to the bed in which velocity information was gathered, were not given. However, we have reason to believe that the structures were similar, especially as the comparative flow patterns were consistent, and as with the cylinder-packed beds, the ability of the methodology to quantitatively predict the local porosity of low aspect ratio ring-packed columns has been demonstrated elsewhere.[32] An example of one of these simulated bed structures, and its adherence to experimentally measured radial voidage data[45] in a bed of equal aspect ratio to that used for flow prediction, is presented in Figure 2. The fundamental difference between the two ring-packed beds considered is the respective diameters of the hollow section of the pellets. While the pellets packed in bed "Ring 1" are marginally larger than those in bed "Ring 2" (Table 1), the hole diameters account for 50% and 75%, respectively, of the total particle diameters of the two packing materials. This difference is believed to account for the significant differences between the voidage results, namely, the voidage in the bulk of bed "Ring 1" (0.38) is significantly lower than that of the second bed (0.68). The other noticeable difference is the voidage fluctuation. In "Ring 1," it is much less pronounced than in bed "Ring 2," where the sinuous wave is more clearly defined, especially for the first $2.0d_p$ from the wall. For both cases, however, the predicted bed structure, in terms of radial voidage, closely resembles that of the experimentally derived results.

Figure 2 also presents the averaged velocities for flow through the ring-packed beds with $d_t/d_p = 5.0$ and 10.0. The normalized maximum velocities for the different ring-packings cannot be compared with each other because of the

different inner void fractions of the pellets (Table 1). Unlike the cylindrical packing material, the correlation between radial voidage and fluid velocity is not as clear cut for the ring-packed beds shown in Figure 2, especially for "Ring 1." The most probable reason for this is the different origins of the structural data and the respective flow data. For both ring-packed beds, a minimum local velocity is seen to exist at approximately one particle diameter from the wall, with a maxima at $0.5d_p$, suggesting that peak flow rates exist through the center of the particles. These maximum velocity peaks, however, are much more accentuated than those of the corresponding local voidage peaks, suggesting that channeling effects are more significant in these beds, particularly in near-wall regions despite the voidage values not oscillating to the same extent. This is believed to be due to the orientation of the pellets within the packing. As the external geometry of these pellets is equilateral, the exact position and orientation that they occupy within the bed structure does not have a significant effect on local voidage, provided they are closely packed (i.e., end-to-end, side-to-side or end-to-side, etc.). For the subsequent fluid flow, however, as the pellets are open ended, particle orientation can have a significant impact in terms of resistance to flow and the associated fluid hold-up. Observation of the simulated packed structures showed that the majority of the pellets close to the wall were arranged in such a manner that they were orientated in a near upright position, that is, with holes parallel to the direction of flow. This goes some way to accounting for the high velocities in this region, which would necessarily have been lower had these internal flow channels been blocked.

In general, predicted velocity results for the ring-packed beds are in reasonable qualitative agreement with measured flow data[41,42] with the radial location of velocity maxima and minima seen to correlate well for both beds, and with the predicted velocity magnitude in close agreement with measurements in these regions. Some minor discrepancies in velocity distribution are, however, observed between prediction and experiment for the Raschig ring-packed beds. For "Ring 1," the predicted flow data exceed the measured minimum and maximum peak velocity values[43] with a mean difference in values at these three points ($0.5d_p$ $1.0d_p$, and $1.4d_p$) of 13%. In the second bed, "Ring 2," for measured results,[42] the difference between model prediction is even more exaggerated close to the wall ($\leq 0.6d_p$, mean difference = 22.9%). Beyond $0.7d_p$, however, the two sets of velocity results are reasonably matched, with a mean error of 6.7% to $2.5d_p$. There is good agreement with reported data[42] at radial distances $\leq 2.5d_p$. Beyond this distance from the wall, however, there is again a large degree of scatter, as was observed in the cylinder-packed bed (Cylinder 2).

Analysis of trilobe-packed structures

Comparative packing and flow data for trilobe pellets is presented in Figure 3. A significantly larger aspect ratio (30.8) is reported than for previous structures (Figures 1 and 2), although analysis in the near-wall region is still the main focus. As with the previous two reported packing materials, the predicted dimensionless radial velocity profile follows the trend of the radial voidage. There is good agreement between measured[45] and predicted radial voidage data. A considerably reduced wall effect exists compared with the reported cylinder- and ring-packed structures (Figures 1 and 2), which can be attributed to the higher aspect ratio and the shape of the pellets, which are able pack in much closer contact than the "rounded" pellets (cylinders/rings). From the outer wall, a single dip in porosity (a minimum value of predicted and measured results of 0.468 (0.426) is observed, respectively) is followed by a peak of 0.506 (0.508) at 0.82 particle diameters from the wall. Beyond $1.25d_p$, an essentially uniform voidage profile exists toward the center of the container, with the minor fluctuating differences between measured and predicted data attributable to the random nature of the packing in the central region of the bed. For the corresponding fluid velocity, qualitative agreement is observed with measured data.[45] Below 1.0 particle diameter from the wall, a higher than average predicted fluid velocity (compared with rest of the bed) occurs, with a maximum value at $0.23d_p$ before reaching a minimum value at $0.70d_p$ for measured (MRI) and $0.85d_p$ for predicted. As with the previous examples (Figures 1 and 2), dimensionless radial flow velocity correlates well with corresponding radial voidage data, where in this case a mildly fluctuating flow distribution within the bulk of the bed exists for both measured and predicted flow results, attributed to the randomly arranged voidage channels within the trilobe-packed structure. For Figure 3 a higher flow rate for measured data than for simulated results is also observed, which is likely due, in part, to the LBM version used in the present simulations not considering inertial effects. This is observed most clearly where large pore spaces exist within the packing structure, such as in the near-wall region.

In addition to the previously discussed limitations (experimental methodology, data collection, and model limitations), the differences between measured and predicted data can be attributed to the complicated structure of the flow around, and in the case of the rings, through the randomly packed particles within the packed structures. There is also a degree of error associated with the simulation methods, as digital rotation does not completely preserve the number of solid voxels making up an object. This error, however, is usually $<1\%$ and nonaccumulative, and is therefore relatively easy to quantify. The assessment of other secondary effects is more complicated. For instance, particle rotation can make an otherwise smooth surface full of "staircases," and vice versa. The degree of roughness created in this manner changes every time a particle is rotated. Only a single dislocated voxel is needed to upset the local structure. If a dislocated voxel "sticks out," it creates a one-pixel wide gap. Conversely, if dislocated voxels create indented areas or holes, part of another object may fill in the gap. LBM simulations are highly dependant upon particle resolution. Therefore, it is clear that inputting such structures, containing minute individual inaccuracies caused by particle rotation, yet which are unquantified on a global scale, into LBM will cause subsequent inaccuracies in fluid flow predictions. However, as has been demonstrated, the structural packing and fluid flow models provide results that are qualitatively comparable to experimentally analyzed low aspect ratio beds, and that are generally in reasonable quantitative agreement. This means that for trending exercises, this associated error is small, and does not adversely affect the results from providing qualitatively accurate predictions.

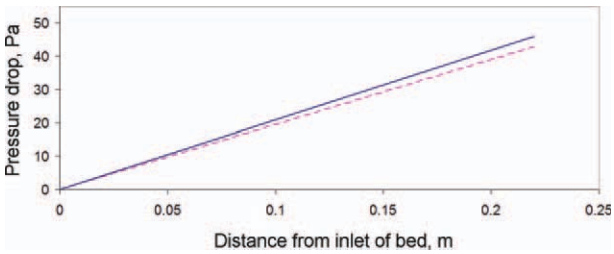

Figure 4. Comparison of pressure drop through a bed of monodispersed spheres, $d_t/d_p = 3.0$, Re = 4.

(Dashed line – Ref. 47; solid line – LBM prediction). [Color figure can be viewed in the online issue, which is available at wileyonlinelibrary.com.]

From Figures 1 and 2, the measured normalized maximum velocity in the vicinity of the wall increases very little with changing particle diameter, d_p. Typically, beds with lower aspect ratios lead to larger gaps at the container wall, which in turn leads to less resistance to flow and so greater channeling effects in these areas. This manifestation of a higher dimensionless velocity at the wall is not observed between the respective beds considered, however, which leads to the theory that this effect only becomes significant when comparing beds of large aspect ratio with beds of much smaller d_t/d_p values. For beds of typically low aspect ratio, differences between d_t/d_p values, even where relatively large such as in Figure 2 (with $d_t/d_p = 5.0$ and $d_t/d_p = 10.0$), have little impact in terms of different flow velocities at the wall.

Pressure drop results

For fixed bed reactors, pressure drop is a significant characteristic in their effective design and operation,[46] where correlations based on experimental data are widely utilized. However, these equations, as with those used to predict bed structure, are limited by the range of information used in their creation and the often simplified assumptions upon which they are based. In this study, the LBM used was a constant pressure-gradient model. Therefore, simulated pressure drop versus distance is expected to be a straight line. If experimental results also show a straight line, it means the creeping flow conditions (Darcy's law regime) are met.

For the mean simulation result reported (Figure 4), a single-phase, saturated liquid flow was passed through a set of three packings of uniform spherical particles, generated as described in "Numerical Simulation Methods" section. The decrease in fluid pressure is compared with that of an experimentally measured bed,[47] with both structures having an aspect ratio (d_t/d_p) of 3.0 and equivalent packing heights ($12d_p$). The flow through these random packings was simulated for a single Reynolds number of 4. A linear relationship exists between pressure drop and distance in the direction of flow in the bed.

Flow field analysis

The simulated three-dimensional flow fields occurring in packed beds for the case of cylinders ($d_t/d_p = 8.3$), Raschig rings ($d_t/d_p = 5.0$), and trilobe pellets ($d_t/d_p = 30.8$) are shown in Figure 5. The LBM simulations were undertaken

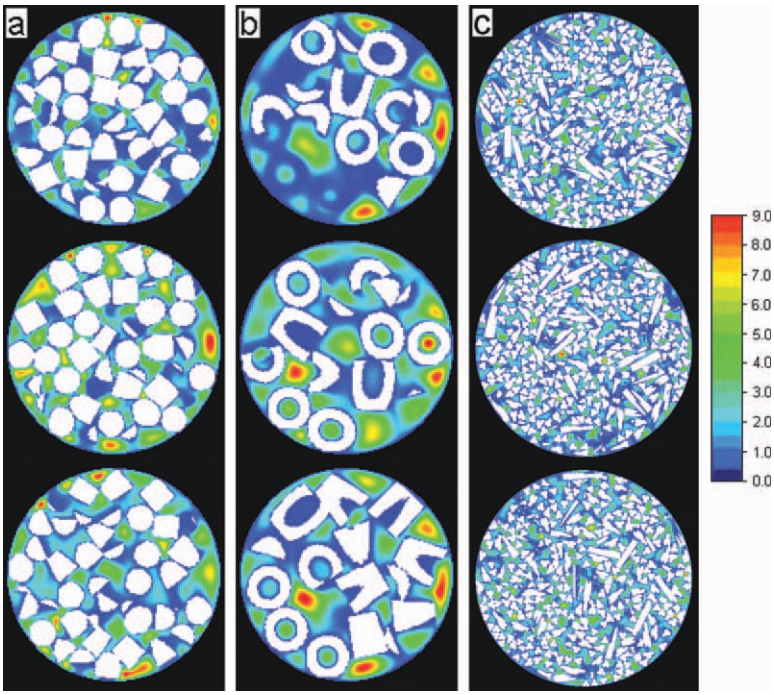

Figure 5. Cross-sectional images of fluid flow through; (a) cylinder-packed ($d_t/d_p = 8.3$); (b) ring-packed ($d_t/d_p = 5.0$); and (c) trilobe-packed bed ($d_t/d_p = 30.8$) at inlet (top), center (middle), and outlet (bottom) of column (scale bar shows normalized velocity scale).

[Color figure can be viewed in the online issue, which is available at wileyonlinelibrary.com.]

in a three-dimensional cylindrical vessel with dimensions of $400 \times 400 \times 250$ voxels (following 1/4 of the total column height removed from end to exclude either inlet or outlet regions). Three contour plots of the axial velocities for several cross sections of each bed are given. The images were obtained from below the first layer of particles (top), the central section (middle), and from above the final layer of pellets (bottom).

Variations in fluid flow velocities (Figure 5) exist because of the varying packing densities, as partly demonstrated by the radial porosity distributions of Figures 1–3. The method of flow field analysis, however, allows for clearer understanding of fluid behavior within different bed types, where flow distribution develops based on the free channels within the matrix. The algorithm output allows for an accurate, pixel-by-pixel, examination of results along the whole length of the bed, from inlet to outlet, providing a straightforward method of examining the changing flow distribution within the bed structure.

From Figure 5b, a relatively high velocity exists through the center of the ring pellets, confirming the simulation and experimental profiles given in Figure 2, where the peak velocity, due to channeling, is observed at $0.5d_p$ from the wall. This contrasts to the results for cylinder and trilobe packings where these maxima occur for both beds at a distance from the wall corresponding to $0.2d_p$ and $1.0d_p$ (Figures 1 and 3). Along the height of each bed, fluid channeling is clearly observed (Figure 5), and in localized areas, mainly in the near-wall regions, peak fluid velocity is as much as nine times greater than the velocity measured in other areas of the bed. By contrast, the averaged radial profiles considered for the same beds in previous figures (Figures 1–3) display significantly lower peak velocities of $\sim$0.35–1.9 times that of the baseline superficial velocity.

Conclusions

The collision guided digital packing algorithm (DigiCGP) has been demonstrated, by comparison with experimental data, to be capable of predicting the detailed geometrical structures of a range of packed columns, and the corresponding bulk and local porosity distributions compare well with those data. The resulting complex structures were then used as the basis of flow simulations using LBM. Dimensionless velocity profiles, normalized against the superficial velocity measured inside the empty tubes, were obtained for monodisperse packings of cylinders, Raschig rings, and trilobe pellets by averaging over several thousand local results for the axial flow component within each cross section. Representative flow profiles, obtained by further averaging these results over several repackings, were used to determine the reproducibility of the voidage and velocity results for different particle shapes and diameters, with reasonable agreement with experimental data being observed. The results show fluid channeling close to walls, with averaged maximum velocities in this region that are in qualitative agreement with experimental observations. Overall, the combined modeling approach used leads to better understanding of the hydrodynamics of flow through specific porous structures, which should be of benefit to the improved design and operation of fixed bed systems.

Literature Cited

1. Jiang Y, Khadilkar MR, Al-Dahhan MH, Dudukovic, MP. Single phase flow modelling in packed beds: discrete cell approach revisited. *Chem Eng Sci*. 2000;55:1829–1844.
2. Taylor K, Smith A, Ross S, Smith M. CFD modelling of pressure drop and flow distribution in packed bed filters. *Phoenics J Comput Fluid Dyn Appl*. 2000;13:399–413.
3. Jiang Y, Khadilkar MR, Al-Dahhan MH, Dudukovic MP. CFD modelling of multiphase flow distribution in catalytic packed bed reactors: scale down issues. *Catal Today*. 2001;66:209–218.
4. Zeiser T, Lammers P, Klemm E, Li YW, Bernsdorf J, Brenner G. CFD-calculation of flow, dispersion and reaction in a catalyst filled tube by the lattice Boltzmann method. *Chem Eng Sci*. 2001;56: 1697–1704.
5. Dixon AG, Nijemeisland M, Stitt EH. Packed tubular reactor modelling and catalyst design using computational fluid dynamics. *Adv Chem Eng*. 2006;31:307–315.
6. Maier RS, Kroll DM, Bernard RS, Howington SE. Pore-scale simulation of dispersion. *Phys Fluids*. 2000;12:2065–2079.
7. Freund H, Bauer J, Zeiser T, Emig G. Detailed simulation of transport processes in fixed-bed reactors. *Ind Eng Chem Res*. 2005;44: 6423–6434.
8. Hlushkou D, Khirevich S, Apanasovich V, Seidel-Morgenstern A, Tallarek U. Pore-scale dispersion in electrokinetic flow through a random sphere packing. *Anal Chem*. 2007;79:113–121.
9. Freund H, Zeiser T, Huber F, Klemm E, Brenner G, Durst F, Emig G. Numerical simulations of single phase reacting flows in randomly packed fixed-bed reactors and experimental validation. *Chem Eng Sci*. 2003;58:903–910.
10. Sullivan SP, Sani FM, Johns ML, Gladden LF. Simulation of packed bed reactors using lattice Boltzmann methods. *Chem Eng Sci*. 2005; 60:3405–3418.
11. Haughey DP, Beveridge GSG. Structural properties of packed beds—a review. *Can J Chem Eng*. 1969;47:130–140.
12. Lerou JJ, Froment GF. Velocity, temperature and conversion profiles in fixed bed catalytic reactors. *Chem Eng Sci*. 1977;32:853–861.
13. Lerou JJ, Froment GF. The measurements of void fraction profiles in packed beds. *NATO ASI Ser E: Chem Reactor Des Technol*. 1986; 110:853–861.
14. Daszkowski T, Eigenberger G. A re-evaluation of fluid flow, heat transfer and chemical reaction in catalyst filled tubes. *Chem Eng Sci*. 1992;47:2245–2250.
15. Papageorgiou JN, Froment GF. Simulation models accounting for radial voidage profiles in fixed-bed reactors. *Chem Eng Sci*. 1995;50: 3043–3056.
16. Ridgway K, Tarbuck KJ. Radial voidage variation in randomly-packed beds of spheres of different sizes. *J Pharm Pharmacol*. 1966;18: 168S–175S.
17. Goodling DS, Vachon RI, Stelpflug WS, Ying SJ, Khader S. Radial porosity distribution in cylindrical beds packed with spheres. *Powder Technol*. 1983;35:23–29.
18. Froment GF, Bischoff KB. *Chemical Reactor Analysis and Design*, 5th ed. New York: Wiley & Sons Inc., 1990.
19. Martin H. Low Peclet number particle-to-fluid heat and mass transfer in packed beds. *Chem Eng Sci*. 1988;33:913–919.
20. Cohen Y, Metzner AB. Wall effect in laminar flow of fluids through packed beds. *AIChE*. 1981;27:705–715.
21. Mueller GE. Radial void fraction distributions in randomly packed fixed beds of uniformly sized spheres in cylindrical containers. *Powder Technol*. 1992;72:269–275.
22. Seidler GT, Martinez G, Seeley LH, Kim KH, Behne EA, Zaranek S, Chapman BD, Heald SM. Granule-by-granule reconstruction of a sandpile from X-ray microtomography data. *Phys Rev E*. 2000;62: 8175–8182.
23. Richard P, Philippe P, Barbe F, Bourlès S, Thibault X, Bideau D. Analysis by X-ray microtomography of a granular packing undergoing compaction. *Phys Rev E*. 2003;68:020301.
24. Aste T, Saadatfar M, Sakellariou A, Senden TJ. Investigating the geometrical structure of disordered sphere packings. *Physica A*. 2004; 339:16–23.
25. Zhang W, Thompson KE, Reed AH, Beenken L. Relationship between packing structure and porosity in fixed beds of equilateral cylindrical particles. *Chem Eng Sci*. 2006;61:8060–8074.

26. Kutsovsky Y. Nuclear magnetic resonance imaging of flow and dispersion in bead packs, PhD Thesis. University of Minnesota, 1996.
27. Sharma S, Mantle MD, Gladden LF, Winterbottom JM. Determination of bed voidage using water substitution and 3D magnetic resonance imaging, bed density and pressure drop in packed bed reactors. *Chem Eng Sci*. 2001;56:587–595.
28. Nandakumar K, Shu Y, Chuang KT. Predicting geometrical properties of random packed beds from computer simulation. *Am Inst Chem Eng J*. 1999;45:2286–2294.
29. Abreu CRA, Tavares FW, Castier M. Influence of particle shape on the packing and on the segregation of spherocylinders via Monte Carlo simulations. *Powder Technol*. 2003;134:167–180.
30. Maier RS, Kroll DM, Bernard RS, Howington SE, Peters JF, Davis HT. Hydrodynamic dispersion in confined packed beds. *Phys Fluids*. 2003;15:3795–3815.
31. Malinouskaya I, Mourzenko VV, Thovert J-F, Adler PM. Random packings of spiky particles: geometry and transport properties. *Phys Rev E*. 2009;80:011304.
32. Caulkin R, Ahmad A, Fairweather M, Jia X, Williams RA. Digital predictions of complex cylinder packed columns. *Comp Chem Eng*. 2009;33:10–21.
33. Caulkin R, Jia X, Xu C, Fairweather M, Williams RA, Stitt H, Nijemeisland M, Aferka S, Crine M, Léonard A, Toye D, Marchot P. Simulations of structures in packed columns and validation by X-ray tomography. *Ind Eng Chem Res*. 2009;48:202–213.
34. Jia X, Williams RA. A packing algorithm for particles of arbitrary shapes. *Powder Technol*. 2001;120:175–186.
35. Wolf-Gladrow DA. *Lattice-Gas Cellular Automata and Lattice Boltzmann Models*. Berlin: Springer-Verlag, 2000.
36. Caulkin R, Jia X, Fairweather M, Williams RA. Lattice approaches to packed column simulations. *Particuology* 2008;6: 404–411.
37. Succi S. *The Lattice Boltzmann Equation for Fluid Dynamics and Beyond*. UK: Oxford Science Publications, 2001.
38. Qian YH, d'Humieres D, Lallemand P. Lattice BGK model for Navier–Stokes equation. *Europhys Lett*. 1992;17:479–484.
39. Martys N, Chen H. Simulation of multi-component fluids in complex three-dimensional geometries by the lattice Boltzmann method. *Phys Rev A*. 1996;53:743–752.
40. Winterberg M, Tsotsas E, Krischke A, Vortmeyer D. A simple and coherent set of coefficients for modelling of heat and mass transport with and without chemical reaction in tubes filled with spheres. *Chem Eng Sci*. 2000;55:967–979.
41. Bey O, Eigenberger G. Fluid flow through catalyst filled tubes. *Chem Eng Sci*. 1997;52:1365–1376.
42. Giese M, Rottschäfer K, Vortmeyer D. Measured and modelled superficial flow profiles in packed beds with liquid flow. *AIChE*. 1998; 44:484–490.
43. Mantle MD, Sederman AJ, Gladden LF. Single- and two-phase flow in fixed-bed reactors: MRI flow visualisation and lattice-Boltzmann simulations. *Chem Eng Sci*. 2001;56:523–529.
44. Sharma S, Mantle MD, Gladden LF, Winterbottom JM. Determination of bed voidage using water substitution and 3D magnetic resonance imaging, bed density and pressure drop in packed-bed reactors. *Chem Eng Sci*. 2001;56:587–595.
45. Roshani S. Elucidation of local and global structural properties of packed bed configurations, PhD Thesis. University of Leeds, 1990.
46. Foumeny EA, Benyahia F, Castro JAA, Moallemi HA, Roshani S. Correlations of pressure drop in packed beds taking into account the effect of containing wall. *Chem Eng Sci*. 1993;36:536–540.
47. Jamialahmadi M, Müller-Steinhagen H, Izadpanah MR. Pressure drop, gas hold-up and heat transfer during single and two-phase flow through porous media. *Int J Heat Fluid Flow*. 2005;26:156–172.

Manuscript received Nov. 30, 2009, revision received Dec. 14, 2010, and final revision received May 20, 2011.